Full length article

Differentiation and traffic of IgM+ B cells between focal dark spots in skeletal muscle of Atlantic salmon, lymphoid and adipose tissues

Raúl Jiménez-Guerrero [a,*], Christian Karlsen [b], Pierre Boudinot [c], Sergey Afanasyev [d], Turid Mørkøre [a], Aleksei Krasnov [b]

[a] *Department of Animal and Aquacultural Sciences, Norwegian University of Life Sciences, Ås, Norway*
[b] *Department of Fish Health, Nofima, Ås, Norway*
[c] *Université Paris-Saclay, INRAE, UVSQ, VIM, Jouy-en-Josas, France*
[d] *Sechenov Institute of Evolutionary Physiology and Biochemistry, Saint Petersburg, Russia*

ARTICLE INFO

ABSTRACT

Focal dark spots (DS) in farmed Atlantic salmon fillets contain a significant number of B cells as revealed by the high abundance of immunoglobulin (Ig) transcripts in transcriptome data. The immune response in DS remains unknown while they represent a major problem in commercial aquaculture. Here, we characterized the diversity and clonal composition of B cells in DS. Sixteen gene markers of immune cells and antigen presentation were analyzed with RT-qPCR. All genes expression showed a positive correlation with DS area and intensity. The flatter the DS, the higher the expression of *cd28, csfr, ctla, igt*, and *sigm*, the lower expression of *cd83* and *btla*, and the larger the cumulative frequency within DS. The expression of most of the analyzed immune genes, including three Ig types and markers of B cells was lower in DS than in the lymphatic organs, head kidney and spleen, but significantly higher compared to skeletal muscle. High levels of *ctla4* and *cd28* in DS might indicate the recruitment of T cells. Sequencing of IgM repertoire (Ig-seq) assessed migration of B cells by co-occurrence of identical CDR3 sequences in different tissues. The combination of gene expression and Ig-seq revealed the presence of several stages of B cell differentiation in DS. B cells at the earliest stage, with high ratio of membrane to secretory IgM (*migm* and *sigm*), showed minor Ig repertoire overlap with other tissues. Further differentiation stage (increased *sigm* to *migm* ratio and high expression of *pax5* and *cd79*) was associated with active movement of B cells from DS towards lymphatic organs and visceral fat. Traffic and expression of immune genes decreased at later stages. These B cells could be involved in a response directed against viruses, pathogenic or opportunistic bacteria in DS. Seven of eight fish were positive for salmon alphavirus, and levels were higher in DS than in unstained muscle. PCR with universal primers to the 16S rRNA gene did not detect bacteria in DS. Although the evolution of DS most likely implies local exposure to antigens, neither this nor previous studies have found a necessary association between DS and pathogens or self-antigens.

1. Introduction

Focal dark spots (DS) are red and black discolorations responsible of the major quality problem in farmed Atlantic salmon (*Salmo salar* L.), affecting about 16–18% of harvest size salmon [1]. Transcriptome profiling of DS suggested trauma as a possible etiology [2], and a recent study found a relationship between DS and damaging incidents in the rib cage [3]. Hemorrhages or red (early) DS are changes associated with a pro-inflammatory micro-environment and M1 type macrophages, while M2 type macrophages were dominating in black DS [4]. Histopathology

of DS finds varying numbers of erythrocytes, inflammatory cells, and fibrous infiltrations in different forms of chronic-active inflammatory processes [5]. Moreover, black DS typically contain abundant T cells, and MHC class I and II+ cells [4,6]. Transcriptome analysis revealed the presence of many B cells [2], which besides from antibody/immunoglobulin (Ig) production, might be involved in immunoregulation [7] and tissue repair [8]. The co-localization of immune responses with *Piscine orthoreovirus*-1 (PRV-1) [4,5] suggests possible intervention of pathogens in DS development.

B cells are defined as antibody-producing cells. In human and mouse,

---

following activation by antigen, B cells can differentiate into antibody-secreting cells, specifically, short lived plasmablasts that divide and long lived plasma cells that do not proliferate [9], as well as memory B cells, which are long-lived membrane-bound Ig cells that quickly respond to antigen upon recall [10]. In the last decade, different subsets of regulatory B cells have also been identified. In particular, plasma cells with immune regulatory functions have been described as producing interleukin-10 or interleukin-35 [7]. A first wave of B cell response against pathogens often occurs in a T-independent way, followed by a T-dependent immune response in the spleen (S) and lymph nodes, with the development of the germinal center reaction and production of antibody-secreting cells and memory cells that largely locate in the S and bone marrow [11]. However, other populations of memory B cells are located in multiple tissues with specific signatures, and the role of these tissue-resident memory B cells in protection and adaptive responses has been recently reevaluated [12]. In fish, and in particular in salmonids, both involvement of B cells in inflammatory mechanisms and circulation of responding antibody-secreting cells are poorly understood. In absence of lymph nodes, hematopoietic bone marrow and clear division of S into white and red pulp, the specialized niches of B cells are different [13]. Sequential expression of key transcription factors strongly suggest that B cell differentiation occurs in the pronephros [14], which seems to be also a niche for plasma cells. However, as very few B cell markers are targeted by available monoclonal Igs, it remains very complicated to track B cells involved in responses and inflammatory mechanisms. In this context, IgHmu repertoire comparison across different organs provides an interesting approach.

We previously developed an Ig-seq protocol – sequencing of the junctional region of IgM heavy chain transcripts (i.e., the Complementarity Determining Region (CDR)-3) [15], which led us to discover a migration pattern of B cells assessed by co-occurrence of IgHmu CDR3 sequences expressed in different tissues of the same individual [16]. Each IgHμ CDR3 sequence can be considered as a barcode for a B cell clone. Indeed, a very large diversity of junctional sequences is produced in developing B cell populations by recombination of V, D, and J genes with enzymatic insertions and deletions at joints [17]. Hence, the probability of independent production of identical CDR3 sequences is low. Such events may occur mainly for rearrangements in which no or very few nucleotides are added to the germline sequences [18]. Therefore, co-occurrence of IgHμ CDR3 sequences in different tissues or sites is generally explained by the migration of B cells belonging to the same clone, *i.e.,* deriving from a common precursor. Our previous reports suggested that traffic increases under various conditions, such as smoltification [19], vaccination, and viral infections [20].

In this work, we propose to use IgHmu CDR3 sequences (i.e., the region encoding IgHm CDR3) to track B cell clones across different tissues, which are potentially relevant for the development of DS. Combined with other markers, including the three Ig isotypes, master regulators of B cell differentiation, markers of antigen presentation, T cells, and macrophages analyzed with RT-qPCR, we present the first geographic analysis of B cells recirculation between DS and other niches for lymphocytes that are potentially important in the development/evolution of the event. We also attempted to detect and characterize bacteria and viruses in DS.

2. Materials and methods

2.1. Fish material

Non-sexually mature and externally healthy Atlantic salmon (average weight 4.5 kg) from a commercial-scale research and development (R&D) facility were used [3]. The salmon were sampled immediately after slaughtering (electrical stunning and bleeding), and eight fish were selected for further analyses based on clearly visible DS through the parietal peritoneum. Each selected fish was sampled for head kidney (HK), S, and visceral peritoneum fat (VF) (one sample per tissue from each fish). Samples were stored in RNAlater solution (Thermo Fisher Scientific, Waltham, MA, USA). Pictures of the DS were taken before and after the removal of the parietal peritoneum and ribs, using a Canon PowerShot G7 X Mark II (Canon Inc., Tokyo, Japan), 5472×3648 resolution, "Auto" mode, flash off, and ambient lighting. Dark-stained tissue from each DS was sampled (three different samples per DS from each fish). Normal skeletal muscle (SM) was sampled from the same anatomical region on the opposite fillet side to the DS (three different samples per opposite side from each fish). Samples were stored in RNAlater solution. The same DS and SM samples were used for RT-qPCR, IgM sequencing, and PCR amplification. DS were visually evaluated using a log - 2 score system based on diameter (1, grey DS < 3 cm; 2, DS < 3 cm; 4, DS 3 – 6 cm), and estimating the relative focal area (myomere^2), intensity level (relative area*darkness), and shape (aspect ratio; horizontal length/vertical length) [3].

2.2. RNA extraction and RT-qPCR

Sixteen selected and a reference gene for RT-qPCR were selected with preference to the markers of antigen presentation (*cd40* and *mhc2*) and cell lineages. Analysis included the three isotypes of salmon Ig: *igd*, *igt* and *igm*. The transition from a membrane to a secretory isoform (*migm* and *sigm*) marks the beginning of antigen–dependent differentiation of naïve B cells into antibody-secreting cells. *Pax5* is essential for commitment of progenitors to B cells [21], while *blimp1* controls their terminal differentiation [22]. The temporal expression patterns of these genes in salmonid fish support their roles [23]. *Cd79* is involved in signaling after binding of antigens by B cell receptors [24]. Tyrosine kinase *blk* is expressed in differentiating and mature B cells, but not in plasma cells [25]. *Btla* (also known as *cd272*) is a negative regulator of B and T cells [26], while *cd28* and especially *ctla* are specific for activated T cells [27]. *Cd83* is a marker of dendritic cells [28], activated B cells and peripheric Tregs, *csfr* and *marco* were included in analysis as markers of macrophages. We used published primers to *blimp1* [29], *cd40, mhc2* [30], *cd83* [31]*, csfr* [32], *igt, igd, migm* and *sigm* [33], *marco* [34] and reference gene *ef1a* [35] (Supplementary 1). Other primers were designed using OligoPerfect Primer Designer (Thermo Fisher Scientific, Waltham, MA, USA) from the same provider.

Gene expression was analyzed in the DS, SM, HK, and S samples. Tissues (5–10 mg) were placed in tubes with 400 μL lysis buffer (Qiagen, Düsseldorf, Germany) and beads, and 20 μL proteinase K (50 mg/mL) was added to each tube. Samples were homogenized in FastPrep 96 (MP Bio-medicals, Eschwege, Germany) for 120 s at maximum shaking speed, centrifuged, and incubated at 37 °C for 30 min. RNA was extracted on Biomek 4000 robot using Agencourt RNAdvance Tissue kit according to the manufacturer's instructions. RNA concentration was measured with NanoDrop One (Thermo Fisher Scientific, Waltham, MA, USA), and quality was assessed with Bioanalyzer 2100 (Agilent, Santa Clara, CA, USA). RNA was treated with DNase I (Thermo Fisher Scientific, Waltham, MA, USA) and cDNA was synthesized using TaqMan Reverse Transcription Reagent (Applied Biosystems, Waltham, MA, USA) and random hexamers. PCR was run in QuantStudio5 real-time quantitative PCR system (Applied Biosystems, Waltham, MA, USA), the reaction mixture contained 4 μL (21 μg/μL) of diluted cDNA, 5 μL SYBR™ Green Master Mix (Applied Biosystems, Waltham, MA, USA), and 1 μL of the forward and reverse primer. The program included heating for 1 min at 95 °C, amplification (1 s at 95 °C, 20 s at 60 °C) and melting curve stage. Each biological sample was run in duplicates for all genes to ensure reproducibility. After subtraction the Ct values of the reference gene, the average ΔCt was calculated for each gene in the entire data set and subtracted from each datapoint.

2.3. IgM sequencing

Analyses were performed in DS, SM, VF, S and HK samples. Synthesis of cDNA was primed with oligonucleotide to the constant region of

Atlantic salmon IgM (TAAAGAGACGGGTGCTGCAG), using SuperScript IV reverse transcriptase (Thermo Fisher Scientific, Waltham, MA, USA) according to the manufacturer's instructions. Libraries were prepared with two PCR reactions. The first PCR amplified cDNA with a degenerate primer TCGTCGGCAGCGTCAGATGTGTATAAGAGACAGTGARGACWC WGCWGTGTATTAYTGTG, which aligns to the 3′-end of all Atlantic salmon VH genes and a primer GTCTCGTGGGCTCGGAGATGTGTA-TAAGAGACAGGGAACAAAGTCGGAGCAGTTGATGA to the 5′-end of CH. Both primers are complementary to Illumina Nextera adaptors. Reaction mixtures (20 µL) included 10 µL 2X Platinum™ Hot Start PCR Master Mix (Thermo Fisher Scientific, Waltham, MA, USA), 0.5 µL of each primer (10 pmol/µL), 8 µL water, and 1 µL template. The second PCR used Nextera™ XT Index Kit v2 (Illumina, San Diego, CA, USA), and the reaction included 2 µL of each primer and 2 µL product of the first PCR. PCR program included heating: 1 min at 94 °C, amplification: 10 s at 94 °C, 20 s at 53 °C, and 20 s at 72 °C (30 cycles in first PCR and 9 cycles in second PCR) and extension: 5 min at 72 °C. DNA concentration of the amplified product was measured with Qubit (Thermo Fisher Scientific, Waltham, MA, USA). Aliquots of libraries were combined and purified twice with PCR clean-up kit (Qiagen, Düsseldorf, Germany). Sequencing was carried out using Illumina MiSeq™ Reagent Kit v3, 150-cycle (Illumina, San Diego, CA, USA). Libraries were diluted to 4 nM and PhiX control was added to 0.8 nM. After the trimming of Illumina adaptors and primers and removal of low quality reads, CDR3 sequences were identified in IgHµ sequences according to the IMGT standards and definition [36], and transferred to a relational database. The frequencies of unique CDR3 sequences represented with at least two reads per 10^5 reads were evaluated. Cumulative frequencies (CF), i.e. the sums of frequencies of the 50, 100, and 500 most expressed CDR3 were calculated. The traffic of B cells was assessed by pairwise comparison of tissues or samples from the same tissue (DS and SM). CF of CDR3 sequences detected in both compared tissues or samples were calculated. The sequences were registered in NCBI SRA (PRJNA966774).

2.4. Targeting prokaryotic DNA and RNA by PCR amplification

Samples from the RT-qPCR were used, both cDNA and a pooled sample of the corresponding RNA. The amplification of 16S rRNA gene was performed in two ways. The first used degenerate versions of the universal bacterial 16S rRNA gene primers 27F (5′- AGRGTTTGA-TYMTGGCTCAG) and 1492R (5′-GGYTACCTTGTTACGACTT), with an expected amplicon of ~1400 bp. The second was with degenerate versions of primers 341F (5′-CCTACGGGNGGCWGCAG) and 785R (5′-GACTACHVGGGTATCTAATCC), with expected amplified fragments of ~440 bp. PCR of the 16S rRNA gene was performed using 150 ng and diluted 15 ng samples, 1 × Phusion Master Mix, 0.5 µmol/L 16S–F primer, 0.5 µmol/L 16S–R primer, in a 50 µL reaction volume. Extracted bacterial genomic DNA was used as positive control. Negative controls included master mix and primers without template, and reagent mix of cDNA. Samples were prepared on ice and amplified in the thermocycler with the block preheated to 98 °C. The reactions were performed using the following cycling conditions: preincubation at 98 °C for 2 min, followed by 32 cycles of denaturation at 98 °C for 10 s, annealing at 55 °C for 15 s, elongation at 72 °C for 60 s, and a final extension step at 72 °C for 3 min. Aliquots of 8 µL of each reaction were visualized on 1.5% (w/v) agarose gel in TBE buffer using SYBR Safe stain (Edvotek Corp. USA). Absence of distinct positive 16S bands indicated low abundance or no live bacteria, except from the positive control of bacterial genomic DNA.

A further attempt used the same sample material but new ≤10 mg tissue from DS (trimmed to include melanin clusters or granulomas), SM, S and HK. Tissue was added to ZR BashingBead Lysis Tubes (0.1 & 2.0 mm, Zymo Reasearch) prefilled with DNA/RNA Shield™ and homogenized with the mechanical bead beater device Precellys®24 (Bertin Technologies) for 1 × 20 s at 5.000 rpm. Further extraction of DNA was performed using the Quick-DNA/RNA Pathogen Miniprep kit (Zymo Research, Irvine, CA) according to the manufacturer's specifications.

The DNA was eluted in ZymoBIOMICS™ DNase/RNase-Free Water and the concentration determined using a Thermo Scientific Nanodrop 2000c. PCR amplification and visualization of the 16S rRNA gene product with primers 27F/1492R was performed as described above using 1 µL of normalized 21 ng/µL concentration of the extracted DNA as template. The reactions were performed using the following cycling conditions: preincubation at 98 °C for 60 s, followed by 32 cycles of denaturation at 98 °C for 10 s, annealing at 59 °C for 15 s, elongation at 72 °C for 60 s, and a final extension step at 72 °C for 2 min.

2.5. Detection of viruses by RT-PCR

Analyses were performed in DS, and SM samples. The presence of viruses infecting skeletal muscle of Atlantic salmon was checked (PatoGen AS, Ålesund, Norway) using RT-PCR. Analyses included piscine myocarditis virus (PMCV), PRV-1, and salmonid alphavirus (SAV).

2.6. Statistics

Data was analyzed with TIBCO Statistica® (v. 14.0, TIBCO Software Inc., Palo Alto, USA), R software (v. 4.0.3, R Core Team, Vienna, Austria), and Microsoft® Excel® software (v. 16.0.12527.21294, Microsoft Corporation, Redmond, USA). Correlation was assessed between gene expression (ΔΔCt values) and squared root of DS characteristics: visual score, relative area, intensity level, and shape. Gene expression in tissues was analyzed with ANOVA followed by Tukey test. SAV levels (Ct values) were compared with paired *t*-test. The significance level was set at $p < 0.05$. The missing values (not detected) were set to 37.
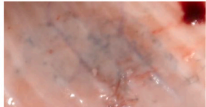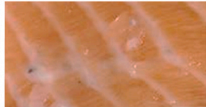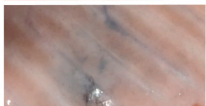
3. Results

3.1. DS description
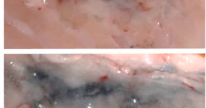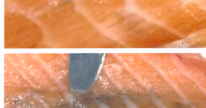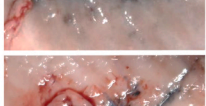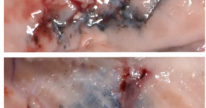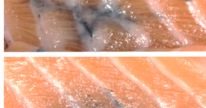
Sampled fish with visible peritoneum discoloration presented DS of different morphologies with a visual color score ranging from 1 to 4 (Fig. 1). All fish presented black DS, excluding fish #4, which presented an apparent combination of red and black DS. The relative area of DS ranged from 0.8 to 4.2 myomere^2. When including the color score, the intensity levels of DS ranged from 2.7 to 16.8. The shape of DS ranged from round (aspect ratio = 1) to very flat (aspect ratio = 8).

3.2. Correlation between gene expression, DS morphology, and CF Spot-Spot

All analyzed immune genes showed a positive correlation ($r \geq 0.42$; $p < 0.05$) between gene expression and DS area and intensity level, especially *mhc2* ($r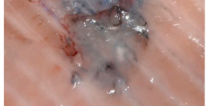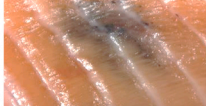 = 0.88$ and 0.82 respectively; $p < 0.001$), *cd83* ($r = 0.81$ and 0.71 respectively; $p < 0.001$) and *igt* ($r = 0.79$ and 0.71 respectively; $p < 0.001$). The flatter the DS, the higher the expression of *cd28, csfr, ctla, igt* ($r \geq 0.22$; $p < 0.05$), and especially *sigm* ($r = 0.57$; $p = 0.02$), the lower expression of *cd83* ($r = -0.34$; $p = 0.01$) and *btla* ($r = -0.31$; $p = 0.04$), and the larger the CF Spot-Spot ($r = 0.5$; $p = 0.02$). There was a positive relationship between *sigm* ($r = 0.85$; $p = 0.005$), *blimp1* expressions ($r = 0.66$; $p = 0.045$), and the CF Spot-Spot.

3.3. Tissue expression of immune genes

Overall, the expression levels of the 16 selected immune genes in DS were intermediate between the lymphatic tissues and SM. Expression of 12 genes was significantly lower in DS than in HK and S and differences were greatest in Ig *(migm, sigm, igd,* and *igt)* and four genes specific for B cells: *pax5, blimp1, blk* and *cd79* (Fig. 2). Possibility of massive recruitment of activated T cells to DS was indicated by expression of *cd28* (higher than in HK) and *ctla4* (increased in comparison with both

ID	PARIETAL PERITONEUM DS	SKELETAL MUSCLE DS	VISUAL SCORE	RELATIVE AREA	INTENSITY LEVEL	SHAPE
1			1	1.4	3.5	5.0
3			2	0.8	2.7	1.0
4			1	3.1	7.9	1.0
5			4	3.6	10.7	8.0
6			2	4.2	16.8	3.0
7			2	2.6	10.2	1.2
8			2	2.7	8.0	4.7
9			4	3.6	14.5	7.8

Fig. 1. Visualization of focal dark spots (DS) in skeletal muscle through parietal peritoneum used for RT-qPCR and Ig-seq. DS are characterized according to visual score (1, grey DS < 3 cm; 2, DS < 3 cm; 4, DS 3–6 cm), relative area (myomere^2), intensity level (relative area*darkness), and shape (aspect ratio; horizontal length/vertical length). DS are ordered according to their ID. Color print.

lymphatic organs). Transcripts of 11 genes including the membrane form of IgM (*migm*), *igd* and *pax5* were more abundant in DS than in SM of the same individual and only *cd40* was expressed at higher levels in SM. The expression of *mhc2* showed no difference between tissues (not included in Fig. 2). Though melanomacrophages are believed to play an important part in the development of DS, expression of *csfr* and *marco* in these areas was not higher than in SM.

3.4. Differentiation stages of DS B cells

Ig-seq in combination with RT-qPCR (Fig. 3) was used to investigate the circulation of B cells at different differentiation stages between DS and other (lymphoid) organs. A total of 90 libraries were sequenced (Supplementary 2). The number of high quality reads, and unique CDR3 nucleotide sequences per samples were respectively 128945 ± 28628 and 5666 ± 1686 (mean ± SD). By CF100, which is inversely related to the repertoire diversity, tissues were divided in two groups: S and HK (6.40‰ and 8.75‰) on the one hand, and VF, DS and normal SM (15.55 – 19.58‰) on the other hand; CF100 in DS was 17.66 ± 1.36‰. As a guide for the assessment of B cells traffic, we suggest a model (Fig. 4. A) that integrates our results with those of our previous studies. The model defines a source tissue (the donor) and a target tissue (the recipient) based on the kinetics of Ig repertoire modifications. In this model, under basal conditions in the absence of recent immunization, the Ig

repertoires are different in each site, *i.e.,* the CF of shared junctional sequences is low. The traffic is stimulated shortly after B cell expansion in the donor (source) tissue. Because migration to a recipient tissue begins with a lag, initial CF is higher in donor tissue. The CF of co-expressed CDR3 sequences gradually grows in the recipient tissue, while in donor tissue the frequency of the corresponding clones decreases. Egress of B cells from donor tissue continues and co-occurrence of junction sequences returns to the basal level. The B cells can reside in recipient tissues for a long time, but their connection with the original organs is not detectable anymore.

The DS from different individual fish were classified according to the stage of differentiation of their B cells (Fig. 3). High level of *migm* and low levels of *sigm* were expressed in DS of fish #4 (Fig. 3. A), suggesting that most B cells had not entered antigen-dependent differentiation into antibody-secreting cells. This was in line with higher expression of genes promoting B cell differentiation (*pax5* and *cd79*). In DS from fish #7 and 9, expression of *migm* was higher or equal to expression of *sigm* and expression of B cells-specific genes (*igd, igt, pax5* and *cd79*) was relatively high. These DS contained B cells which had started an antigen-dependent differentiation into antibody-secreting cells. Fish #5 was most likely at a subsequent stage characterized by an increased *sigm* to *migm* ratio, and lower expression of B cell–specific genes. DS from fish #1, 6, 3 and 8 (Fig. 3. B), ordered by decreasing expression level of *sigm*, still expressed more *sigm* than *migm*, and overall low levels of B cell
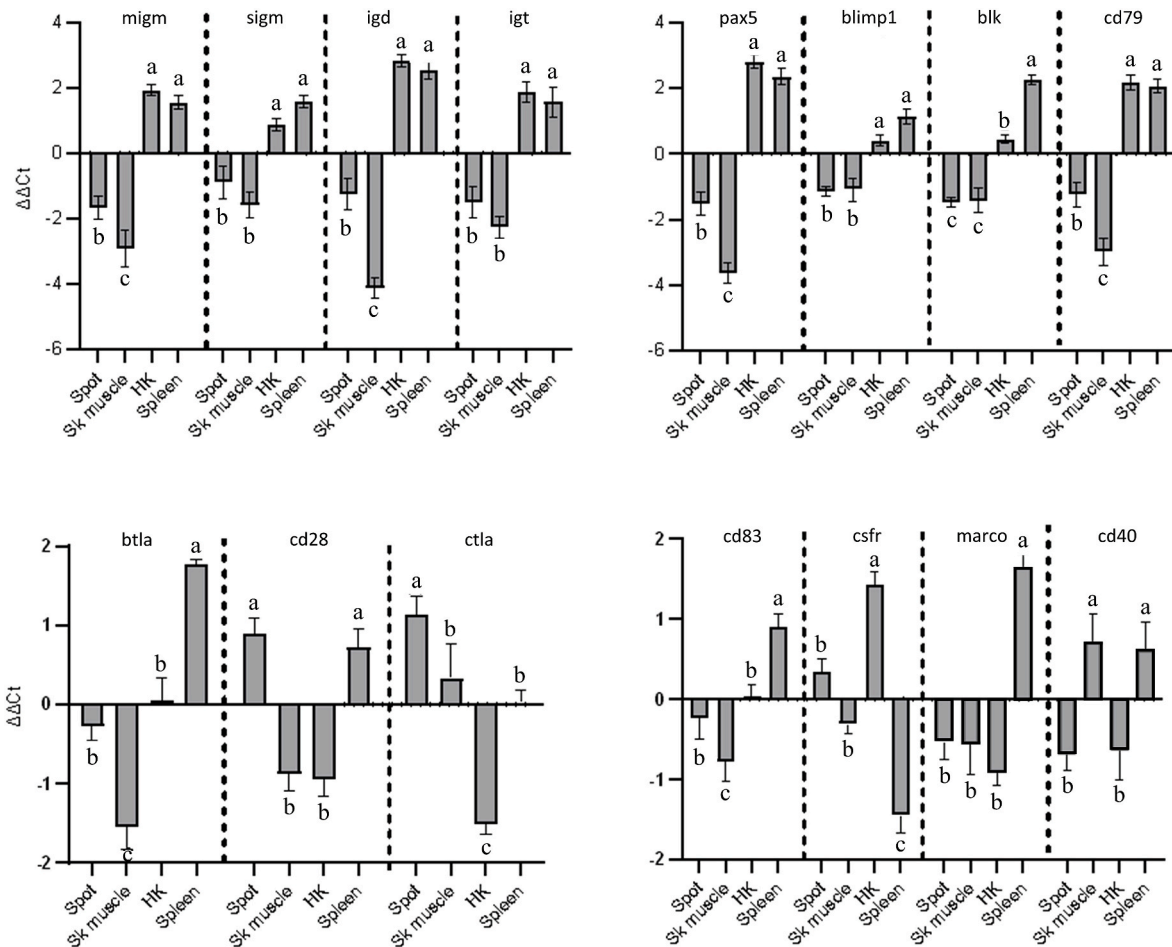
Fig. 2. Expression of immune genes (RT-qPCR). The panel presents genes with differences between tissues. Bars not sharing common letters are significantly different (ANOVA, Tukey test, p < 0.05).

markers (*migm*, *igd*, *igt*, *pax5* and *cd79*) suggesting a reduced amount of B cells likely due to egress.

3.5. CDR3 sharing between organs shed light on B cell recirculation pattern

The abundance of shared IgHm CDR3 between DS and other tissues was used to assess the circulation of B cells within each individual fish. To do so, we identified CDR3 in DS detected in other organs and calculated the cumulative frequencies of shared CDR3, which are represented as bar plots in Fig. 3 (right panels). These CF provide an overview of the fraction of the expressed IgM repertoire corresponding to clones shared by different organs. Sharing across DS from studied fish was analyzed following the differentiation gradient described above.

Spot/spot: The CF of shared CDR3 between the two independent samples from each DS were analyzed as a good measure of the fraction of the whole repertoire they represent. In fish #4, it is the lowest (10%), in a diverse repertoire in which Top frequent CDR3 do not represent a large fraction; The proportion is much higher in DS of fish #9, 7, 5, 1, and 6 (ranging from 30 to 60%), during B cell response while decreased is DS from fish #3 and 8 containing much fewer B cells due to egress towards other sites.

Spot/VF-HK-Spleen: CDR3 from DS of fish #4 are present at very low frequency in other tissues, while they are abundant in VF, HK, and spleen in fish #9, 7, and 5. Interestingly, these clones are particularly frequent in VF, suggesting that this tissue is an important recipient for expanded B cells migrating out of DS. The CF of DS CDR3 present in other tissues is around 10 – 15% in fish #1, 6, 3, and 8, likely

representing the situation post DS B cell responses and egress.

VF-HK-Spleen/Spot: Most frequent CDR3 sequences expressed in VF or HK or spleen were overall less frequent in DS, than CDR3 from DS were in the other organs. An interesting observation, which looks consistent across the putative developmental stages of DS B cells (hence, with fish order in Fig. 3), was that the highest sharing was between VF and DS (see fish #4, 5, 1, 6, 3), suggesting privileged B cell circulation between these tissues.

Overall, our analysis suggests that B cells can expand and mature into antibody-secreting cells within DS, then egress towards lymphoid organs, possibly with a preference for VF (Fig. 4).

3.6. Prokaryotic RNA and DNA, viral RNA

PCR analyses with universal primers found no evidence of bacterial RNA or DNA in DS and SM. All fish were free from PMCV. PRV-1 was detected in fish #5 (normal muscle and DS) and #6 (DS). Fish #6 and normal muscle of fish #2 were SAV negative. SAV was detected in all other samples and in DS its level was significantly higher: 3.9 ± 1.4 (Ct ± SE), p = 0.03, paired *t*-test (Supplementary 3). No relationship was observed between SAV Ct values and DS morphology parameters (score, area, level, and shape), expression of immune genes, and CF Spot-Spot.

4. Discussion

Different hypotheses have been proposed to explain the development of DS in Atlantic salmon. Red DS are most likely initiated by damaging events in the rib cage [3], but the transition from red to black DS still
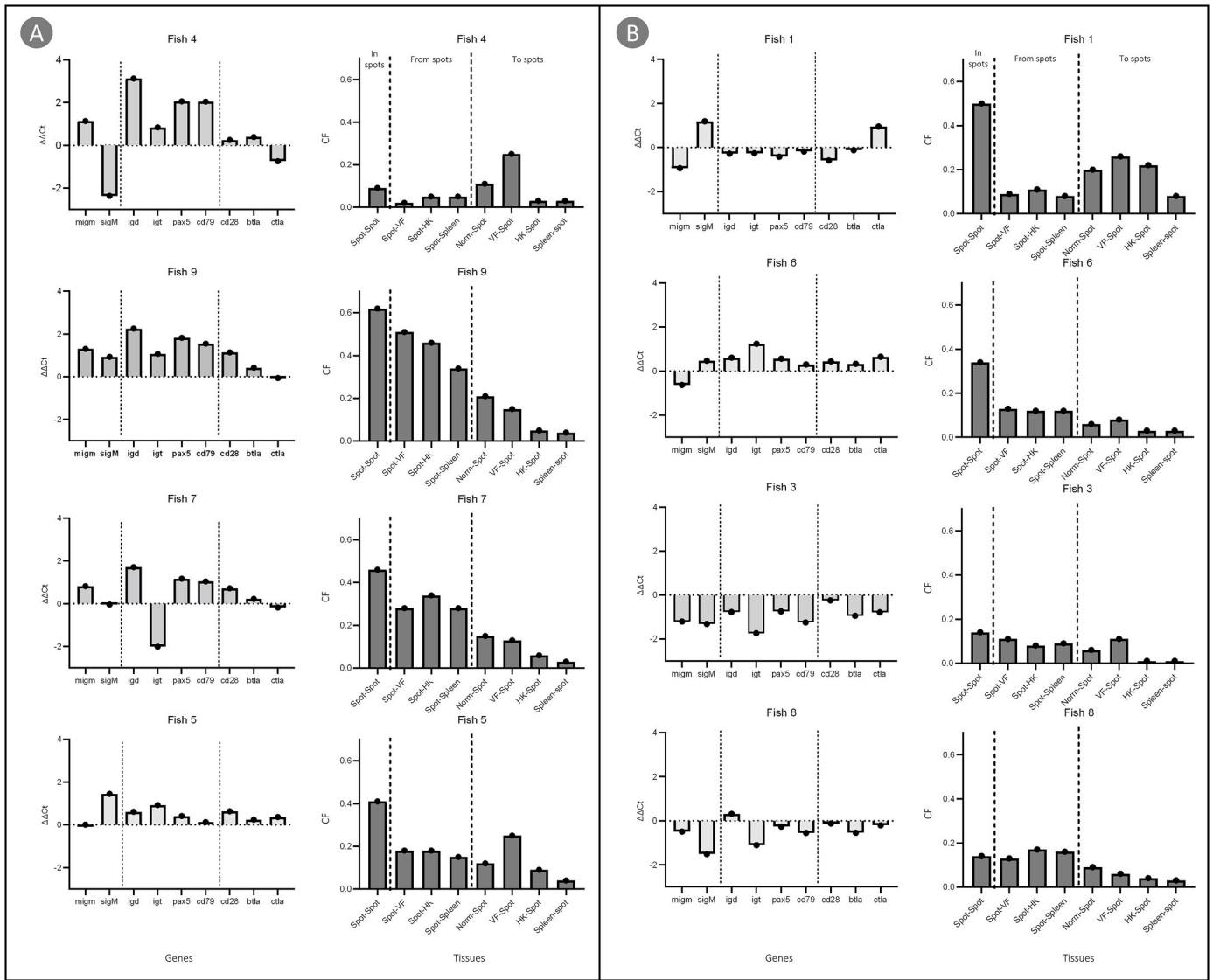
Fig. 3. Association between gene expression in focal dark spots (spots) and co-occurrence of IgM sequences in spots and tissue samples from the same individuals. Fish at early (A), mid and late stages (B) of B cells differentiation in spots: gene expression in spots (left) and cumulative frequencies (CF) of CDR3 sequences detected in spots replicates and pairs of tissues (right). VF – visceral peritoneum fat. HK – head kidney, Norm – normal skeletal muscle. The right panels represent averaged cumulative frequency of CDR3 sequences from a tissue that are expressed in another site. For example, Spot-VF and VF-Spot are cumulative frequencies of CDR3 present in both tissues are calculated in respectively spots and VF. As two independent samples have been sequenced from each spot, the first bar (Spot-Spot) corresponds to the mean of pairwise comparisons of samples from the same spot.

remains unclear. Accumulations of activated B and T cells in DS could be induced by exogenous antigens due to presence of opportunistic bacteria and/or viruses in the lesion. Previously, parallel sequencing detected higher numbers of bacterial 16s RNA transcripts in DS compared to SM from the same fish [2], supporting this first hypothesis. Infection with the PRV-1 has also been involved in the development of DS. However, given the ubiquity of this virus, the absence of DS after experimental inoculation, and the presence of DS in PRV-1 negative fish in this and previous studies [5], the PRV-1 hypothesis is put in doubt. For the same reasons, higher levels of SAV in DS shown in the present study do not mean that this virus is the causative agent, as proven by similar Ct values in all DS phases in different phases, although the presence of SAV may predispose to the development of DS. In another model, traumatic conditions might stimulate macrophages to migrate from the peritoneum to the musculoskeletal injury. These migrating macrophages could be loaded with vaccine antigens and mineral adjuvants coming from the injection site and participate in the maturation of DS [3]. Since DS can develop in non-vaccinated fish [37,38], aberrant processing of vaccine

components as a prerequisite for the development of DS can be also ruled out. Overall, the mechanisms of DS development remain poorly understood. It is possible that different antigens can cause reactions leading to the accumulation of melanin.

In the present work, we analyzed DS from healthy salmon from a commercial population aged 14 months (4.5 kg) after seawater transfer. From these DS samples, we failed to amplify any bacterial RNA or DNA with PCR, indicating there were not association to ongoing bacterial infection. It might be possible that melanomacrophages had remained in skeletal muscle after an infection had been eliminated. Gene expression profiles revealed that DS contained several populations of B cells with different proportions of naïve and Ab–secreting cells and different levels of IgHmu (*sigm/migm*) expression. IgHm CDR3 sequencing further showed that B cells present in DS belong to many clones, and circulate to other issues including VF, S, and HK. Thus, B cells represent an important and complex cellular component of these inflammatory events, with potential consequences on both DS fate and B cell repertoire.

The local environment of DS is characterized by a high density of

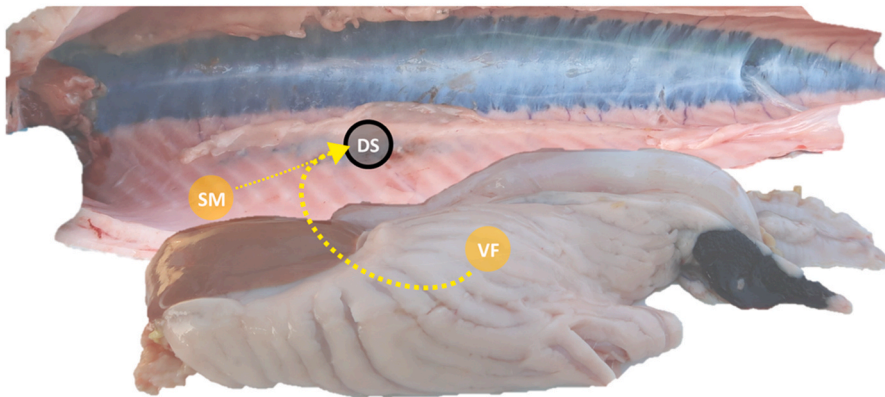**A** Model of B cell trafficking between tissues during the immune response

Definitions:
«**Source**» or «**donor**» tissue: from which B cells egress during the response
«**Recipient**» tissue: into which B cells traffick during the response

Model:
Evolution of CF of most frequent CDR3 (for example, Top100 or shared CDR3) in both source and recipient tissues typically follows a bell shape trajectory during the response. The curve in the recipient tissue is shifted (delayed) from the source tissue by about two days, and the model predicts that B cells move from source to recipient.
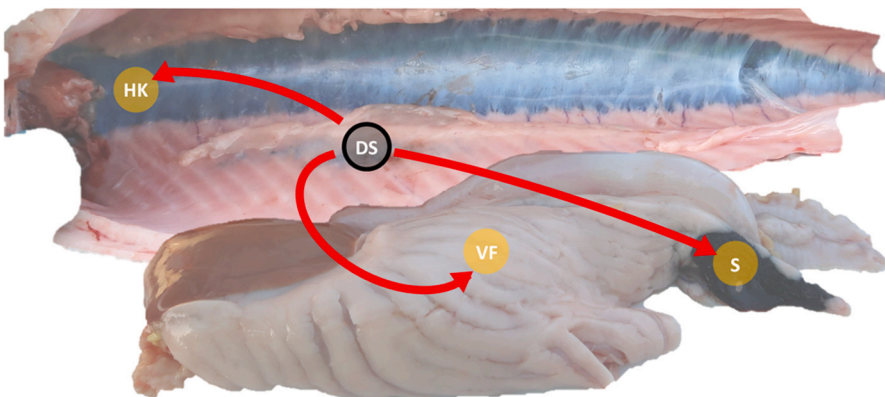
The panel below illustrates the model and the trade off between source and recipent tissues. Each analysed fish is also placed at the the stage of the response suggested by the repertoire analysis.
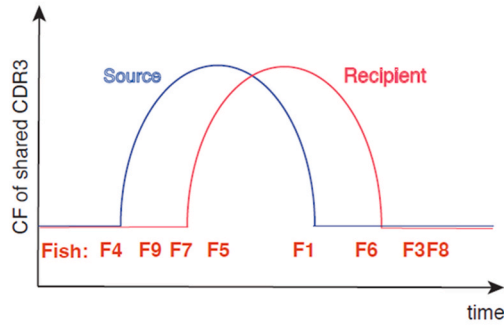
B B cell traffic from tissues to DS

C B cell traffic from DS to other tissues

Fig. 4. Model of B cell traffic in Atlantic salmon between focal dark spots (DS) and other tissues. (A) Model of B cell traffic between a "source" tissue and "recipient" tissue. CF – cumulative frequency. (B) Schematic illustration of B cell traffic. Discontinuous yellow arrows illustrate the likely B cell traffic between tissues before the formation of DS. SM – normal skeletal muscle. VF – visceral peritoneum fat. (C) After exposure to antigens, B cells migrate from DS to other tissues including head kidney (HK), VF and spleen (S) indicating systemic immunization. Continuous red arrows represent the traffic between B cells resident organs or tissues, and DS. The thickness of the arrows indicates the order of shared CF. Based on Fig. 3. Color print.

melanomacrophages, which are involved in antigen processing and presentation [39]. The role of these cells in fish B cell activation and differentiation seems to be complex. In lymphoid organs, it has been proposed that aggregates of melanomacrophages are associated with B cells that express activation-induced cytidine deaminase and undergo somatic hypermutation [40], reminiscent of mammalian germinal centers. However, melanomacrophages are also found in other tissues, especially in the liver in fish, amphibians, and reptiles, and those do not

express activation-induced cytidine deaminase. Incidentally, melano-macrophage centers may also function as focal depositories for intracellular pathogenic bacteria [41], which might explain the associations with bacteria previously reported.

We consider that our data are more in favor of an endogenous path scenario for DS formation [42]. Firstly, there seemed to be an association between DS morphology and the phase of the process, being the CF Spot-Spot and *sigm* expression larger the flatter the DS. Therefore, this points to more B cell activity in flatter DS, which is a link between the type/degree of the initial damage and the immune microenvironment. Secondly, flatter, larger, more intense DS, which is associated with recurrent injury processes [3], also showed higher expression of both innate (macrophage, antigen presentation) and adaptative (B cells, and T helper and cytotoxic cells) immune response genes. Thus, it seems reasonable that continuous mechanical stress in damaged muscle and ribs generates cell damage that may expose lymphocytes to a constant source of autoantigens [43,44] in a pro-activating context leading to melanomacrophage aggregates, where B cells may also acquire a regulatory phenotype driven by local inflammation [45], or respond to tissue regeneration with myoblasts expressing high levels of myositis autoantigens [43,46]. Activation of the immune response in DS in absence of pathogens is in line with the "danger model" proposed by Matzinger [47]. B cells and Ig isolated from DS could be useful for identifying key (auto)antigens involved in DS development in future research. Further transcriptome analysis of DS antibody-producing B cells (with a focus on key factors like BAFF, transcription factors like HIF and TRAF3) might provide insights into their autoimmune phenotype, as reviewed in Mubariki and Vadasz [48].

To gain insight into the involvement of B cells in DS biology, we studied differentiation and traffic of B cells. B cells could enter the antigen-dependent differentiation in the lymphatic tissues and later migrate to DS. Alternatively, B cells might be activated locally, in developing DS in skeletal muscle, and either reside at the site of antigen deposition or migrate to other tissues. We expected preferential migration of B cells from the HK and S to peripheral tissues, including DS. However, our analyses suggested that an antigen stimulated differentiation was rather initiated in DS followed by subsequent migration of cells, a typical finding in inflammatory myopathies in humans [42,49].

We propose here a model (Fig. 4. A) that integrates the conclusions of our data with previous studies [15,19,20]. B cells would recognize their cognate antigen in the DS, start differentiating into antibody-secreting cells and move from DS to other tissues. This model predicts low co-occurrence of clones in different tissues under basal condition and higher CF of shared CDR3 sequences in donor at early phase, and in recipient tissue at late phases. The IgM repertoire in DS with the highest *migm* to *sigm* ratio showed minor overlap with other tissues and co-occurrence of CDR3 sequences was very low even in the replicates from the same area (fish #4 in Fig. 3. A). In fish with relatively high expression of both membrane and secreted IgM in DS, CF of shared CDR3 sequenceswas greater in DS than in other tissues including the S and HK; this suggested co-ordination between antigen stimulated differentiation and traffic of B cells. CF in non-DS samples was higher than in DS in only one individual in concordance with decreased *migm* to *sigm* ratio in DS (fish #1 in Fig. 3. B). Low expression of B cell-specific genes corresponding to the late phase of B cells development coincided with limited sharing. Co-occurrence of CDR3 sequences in DS and VF was greater than in the lymphatic organs indicating that adipose tissue serves as a depot of lymphocytes and can be a transition point in their migration. B cells residing in VF and their responses to vaccination have been characterized in rainbow trout [50] and may constitute a particular B cell population. It will be interesting to investigate the origin and fate of this population, and its relationship with DS B cells. Taken together, our results suggest a local exposure to antigens initiated in melanized foci, which may lead to systemic responsiveness of fish due to active migration of B cells. Thus, if the development of DS is triggered with muscle autoantigens, this might pose a risk of immune-mediate

inflammatory myopathies [42].The phenotype of B cells relocated from DS to other tissues will have to be further characterized to understand their functionality.

5. Conclusion

We show here that B cells traffic between melanized foci and other tissues, implying systemic spreading of clones involved in local DS responses. While the role of DS B cells in the formation of black DS remains unknown, our data provide a new frame to associate B cell responses and maturation with DS evolution. Longitudinal studies starting from the first detection of DS to complete maturation will be important to better understand the mechanisms underlying the development.

CRediT authorship contribution statement

Raúl Jiménez-Guerrero: Investigation, Validation, Formal analysis, Data curation, Resources, Visualization, Writing – original draft, Writing – review & editing. **Christian Karlsen:** Investigation, Validation, Resources, Visualization, Supervision, Writing – original draft. **Pierre Boudinot:** Methodology, Validation, Investigation, Resources, Visualization, Supervision, Formal analysis, Funding acquisition, Writing – original draft, Writing – review & editing. **Sergey Afanasyev:** Investigation, Resources, Validation, Formal analysis, Investigation, Data curation, Funding acquisition, Software. **Turid Mørkøre:** Validation, Formal analysis, Investigation, Resources, Visualization, Supervision, Project administration, Conceptualization, Funding acquisition, Writing – original draft. **Aleksei Krasnov:** Conceptualization, Methodology, Validation, Investigation, Formal analysis, Investigation, Visualization, Supervision, Software, Writing – original draft, Writing – review & editing.

Data availability

Data will be made available on request.

Appendix A. Supplementary data

Supplementary data to this article can be found online at https://doi.org/10.1016/j.fsi.2023.108858.

References

[1] T. Mørkøre, T. Larsson, R. Jiménez-Guerrero, H.M. Moreno, J. Borderias, B. Ruyter, I.B. Standal, A. Sarno, Ø. Evensen, J.-E. Dessen, K.-A. Rørvik, K. Hamre, Ø. Andersen, K. Wakamatsu, S. Ito, K.H. Gannestad, C. Xu, T.-K. Østbye, B. Hillestad, J.S. Torgersen, G. Bæverfjord, EX-Spot, Mørke flekker i laksefilet, Nofima, 2022, p. 78.

[2] A. Krasnov, H. Moghadam, T. Larsson, S. Afanasyev, T. Mørkøre, Gene expression profiling in melanised sites of Atlantic salmon fillets, Fish Shellfish Immunol. 55 (2016) 56–63.

[3] R. Jiménez-Guerrero, G. Baeverfjord, Ø. Evensen, K. Hamre, T. Larsson, J.-E. Dessen, K.-H. Gannestad, T. Mørkøre, Rib abnormalities and their association with focal dark spots in Atlantic salmon fillets, Aquac 561 (2022), 738697.

[4] M.S. Malik, H. Bjørgen, I.B. Nyman, Ø. Wessel, E.O. Koppang, M.K. Dahle, E. Rimstad, PRV-1 Infected macrophages in melanized focal changes in white muscle of Atlantic Salmon (Salmo salar) correlates with a pro-inflammatory environment, Front. Immunol. 12 (2021), 664624.

[5] H. Bjørgen, R. Haldorsen, Ø. Oaland, A. Kvellestad, D. Kannimuthu, E. Rimstad, E.O. Koppang, Melanized focal changes in skeletal muscle in farmed Atlantic salmon after natural infection with Piscine orthoreovirus (PRV), J. Fish. Dis. 42 (6) (2019) 935–945.

[6] H.A. Larsen, L. Austbø, T. Mørkøre, J. Thorsen, I. Hordvik, U. Fischer, E. Jirillo, E. Rimstad, E.O. Koppang, Pigment-producing granulomatous myopathy in Atlantic salmon: a novel inflammatory response, Fish Shellfish Immunol. 33 (2) (2012) 277–285.

[7] D. Catalán, M.A. Mansilla, A. Ferrier, L. Soto, K. Oleinika, J.C. Aguillón, O. Aravena, Immunosuppressive mechanisms of regulatory B cells, Front. Immunol. 12 (2021).

[8] R.F. Sîrbulescu, A. Mamidi, S.-Y.C. Chan, G. Jin, M. Boukhali, D. Sobell, I. Ilieş, J.Y. Chung, W. Haas, M.J. Whalen, A.E. Sluder, M.C. Poznansky, B cells support the repair of injured tissues by adopting MyD88-dependent regulatory functions and phenotype, Faseb. J. 35 (12) (2021), e22019.

[9] S.L. Nutt, P.D. Hodgkin, D.M. Tarlinton, L.M. Corcoran, The generation of antibody-secreting plasma cells, Nat. Rev. Immunol. 15 (3) (2015) 160–171.

[10] I. Dogan, B. Bertocci, V. Vilmont, F. Delbos, J. Mégret, S. Storck, C.A. Reynaud, J.C. Weill, Multiple layers of B cell memory with different effector functions, Nat. Immunol. 10 (12) (2009) 1292–1299.

[11] E. Paramithiotis, M.D. Cooper, Memory B lymphocytes migrate to bone marrow in humans, Proc. Natl. Acad. Sci. U. S. A. 94 (1) (1997) 208–212.

[12] C. Chen, B.J. Laidlaw, Development and function of tissue-resident memory B cells, Adv. Immunol. 155 (2022) 1–38.

[13] H. Bjørgen, E.O. Koppang, Anatomy of teleost fish immune structures and organs, in: K. Buchmann, C.J. Secombes (Eds.), Principles of Fish Immunology : from Cells and Molecules to Host Protection, Springer International Publishing, Cham, 2022, pp. 1–30.

[14] B. Abós, C. Bailey, C. Tafalla, Adaptive immunity, in: K. Buchmann, C.J. Secombes (Eds.), Principles of Fish Immunology : from Cells and Molecules to Host Protection, Springer International Publishing, Cham, 2022, pp. 105–140.

[15] A. Krasnov, S.M. Jørgensen, S. Afanasyev, Ig-seq: deep sequencing of the variable region of Atlantic salmon IgM heavy chain transcripts, Mol. Immunol. 88 (2017) 99–105.

[16] A.F. Bakke, H. Bjørgen, E.O. Koppang, P. Frost, S. Afanasyev, P. Boysen, A. Krasnov, H. Lund, IgM+ and IgT+ B cell traffic to the heart during SAV infection in atlantic salmon, Vaccines 8 (3) (2020).

[17] C.H. Bassing, W. Swat, F.W. Alt, The mechanism and regulation of chromosomal V(D)J recombination, Cell 109 (Suppl) (2002) S45–S55.

[18] M. Yasuike, J. de Boer, K.R. von Schalburg, G.A. Cooper, L. McKinnel, A. Messmer, S. So, W.S. Davidson, B.F. Koop, Evolution of duplicated IgH loci in Atlantic salmon, Salmo salar, BMC Genom. 11 (1) (2010) 486.

[19] H. Lund, A. Bakke, P. Boysen, S. Afanasyev, A. Rebl, F. Manji, G. Ritchie, A. Krasnov, Evaluation of immune status in two cohorts of atlantic salmon raised in different aquaculture systems (case study), Genes 13 (5) (2022).

[20] A.F. Bakke, H. Bjørgen, E.O. Koppang, P. Frost, S. Afanasyev, P. Boysen, A. Krasnov, H. Lund, IgM+ and IgT+ B cell traffic to the heart during SAV infection in atlantic salmon, Vaccines 8 (3) (2020) 493.

[21] C. Cobaleda, A. Schebesta, A. Delogu, M. Busslinger, Pax5: the guardian of B cell identity and function, Nat. Immunol. 8 (5) (2007) 463–470.

[22] S.L. Nutt, K.A. Fairfax, A. Kallies, BLIMP1 guides the fate of effector B and T cells, Nat. Rev. Immunol. 7 (12) (2007) 923–927.

[23] P. Zwollo, Dissecting teleost B cell differentiation using transcription factors, Dev. Comp. Immunol. 35 (9) (2011) 898–905.

[24] P.G. Chu, D.A. Arber, CD79: a review, Appl. Immunohistochem. Mol. Morphol. 9 (2) (2001) 97–106.

[25] S.M. Dymecki, P. Zwollo, K. Zeller, F.P. Kuhajda, S.V. Desiderio, Structure and developmental regulation of the B-lymphoid tyrosine kinase gene blk, J. Biol. Chem. 267 (7) (1992) 4815–4823.

[26] C. Zeng, T. Wu, Y. Zhen, X.P. Xia, Y. Zhao, BTLA, a new inhibitory B7 family receptor with a TNFR family ligand, Cell. Mol. Immunol. 2 (6) (2005) 427–432.

[27] D. Bernard, A. Six, L. Rigottier-Gois, S. Messiaen, S. Chilmonczyk, E. Quillet, P. Boudinot, A. Benmansour, Phenotypic and functional similarity of gut intraepithelial and systemic T cells in a teleost fish, J. Immunol. 176 (7) (2006) 3942–3949.

[28] R.M. Steinman, M. Pack, K. Inaba, Dendritic cells in the T-cell areas of lymphoid organs, Immunol. Rev. 156 (1997) 25–37.

[29] B. Abós, R. Castro, J. Pignatelli, A. Luque, L. González, C. Tafalla, Transcriptional heterogeneity of IgM+ cells in rainbow trout (Oncorhynchus mykiss) tissues, PLoS One 8 (12) (2013), e82737.

[30] L.X. Lagos, D.B. Iliev, R. Helland, M. Rosemblatt, J.B. Jørgensen, CD40L–a costimulatory molecule involved in the maturation of antigen presenting cells in Atlantic salmon (Salmo salar), Dev. Comp. Immunol. 38 (3) (2012) 416–430.

[31] D.B. Iliev, G. Strandskog, M. Sobhkhez, J.A. Bruun, J.B. Jørgensen, Secretome profiling of atlantic salmon head kidney leukocytes highlights the role of phagocytes in the immune response to soluble β-glucan, Front. Immunol. 12 (2021), 736964.

[32] M.M.D. Peñaranda, I. Jensen, L.G. Tollersrud, J.A. Bruun, J.B. Jørgensen, Profiling the atlantic salmon IgM(+) B cell surface proteome: novel information on teleost fish B cell protein repertoire and identification of potential B cell markers, Front. Immunol. 10 (2019) 37.

[33] T.M. Tadiso, K.K. Lie, I. Hordvik, Molecular cloning of IgT from Atlantic salmon, and analysis of the relative expression of τ, μ, and δ in different tissues, Vet. Immunol. Immunopathol. 139 (1) (2011) 17–26.

[34] Y.A. van der Wal, S. Jenberie, H. Nordli, L. Greiner-Tollersrud, J. Kool, I. Jensen, J.B. Jørgensen, The importance of the Atlantic salmon peritoneal cavity B cell response: local IgM secreting cells are predominant upon Piscirickettsia salmonis infection, Dev. Comp. Immunol. 123 (2021), 104125.

[35] K. Julin, L.H. Johansen, A.I. Sommer, Reference genes evaluated for use in infectious pancreatic necrosis virus real-time RT-qPCR assay applied during different stages of an infection, J. Virol. Methods 162 (1–2) (2009) 30–39.

[36] M.-P. Lefranc, The immunologist. https://www.imgt.org/IMGTScientificChart/Nomenclature/IMGT-FRCDRdefinition.html, 1999. (Accessed 7 May 2023).

[37] T. Mørkøre, Mørke Flekker I Laksefilet – Kunnskapsstatus Og Tiltak for Å Begrense Omfanget, 2012. Nofima.

[38] A. Berg, A. Yurtseva, T. Hansen, D. Lajus, P.G. Fjelldal, Vaccinated farmed Atlantic salmon are susceptible to spinal and skull deformities, J. Appl. Ichthyol. 28 (3) (2012) 446–452.

[39] A.E. Ellis, M. de Sousa, Phylogeny of the lymphoid system. I. A study of the fate of circulating lymphocytes in plaice, Eur. J. Immunol. 4 (5) (1974) 338–343.

[40] D. Waly, A. Muthupandian, C.W. Fan, H. Anzinger, B.G. Magor, Immunoglobulin VDJ repertoires reveal hallmarks of germinal centers in unique cell clusters isolated from zebrafish (Danio rerio) lymphoid tissues, Front. Immunol. 13 (2022), 1058877.

[41] C. Agius, R.J. Roberts, Melano-macrophage centres and their role in fish pathology, J. Fish. Dis. 26 (9) (2003) 499–509.

[42] A. Farini, C. Villa, L. Tripodi, M. Legato, Y. Torrente, Role of immunoglobulins in muscular dystrophies and inflammatory myopathies, Front. Immunol. 12 (2021).

[43] N. Kimura, S. Hirata, N. Miyasaka, K. Kawahata, H. Kohsaka, Injury and subsequent regeneration of muscles for activation of local innate immunity to facilitate the development and relapse of autoimmune myositis in C57BL/6 Mice, Arthritis Rheumatol. 67 (4) (2015) 1107–1116.

[44] C. Sciorati, E. Rigamonti, A.A. Manfredi, P. Rovere-Querini, Cell death, clearance and immunity in the skeletal muscle, Cell Death Differ. 23 (6) (2016) 927–937.

[45] S. Fillatreau, Natural regulatory plasma cells, Curr. Opin. Immunol. 55 (2018) 62–66.

[46] T.L. Suber, L. Casciola-Rosen, A. Rosen, Mechanisms of disease: autoantigens as clues to the pathogenesis of myositis, Nat. Clin. Pract. Rheumatol. 4 (4) (2008) 201–209.

[47] P. Matzinger, Tolerance, danger, and the extended family, Annu. Rev. Immunol. 12 (1994) 991–1045.

[48] R. Mubariki, Z. Vadasz, The role of B cell metabolism in autoimmune diseases, Autoimmun. Rev. 21 (7) (2022), 103116.

[49] M. Salajegheh, J.L. Pinkus, A.A. Amato, C. Morehouse, B. Jallal, Y. Yao, S.A. Greenberg, Permissive environment for B-cell maturation in myositis muscle in the absence of B-cell follicles, Muscle Nerve 42 (4) (2010) 576–583.

[50] R. Simón, A. Martín-Martín, E. Morel, P. Díaz-Rosales, C. Tafalla, Functional and phenotypic characterization of B cells in the teleost adipose tissue, Front. Immunol. 13 (2022).